DESIGN OF DIGITAL MULTIPLE MODEL-FOLLOWING INTEGRATED FLIGHT/PROPULSION CONTROL SYSTEMS

B Porter
Department of Aeronautical and Mechanical Engineering
University of Salford
Salford M5 4WT
England

and

X-G Zhang
Flight Automatic Control Research Institute
Chinese Aeronautical Establishment
Xi'an PO Box 41
China

ABSTRACT

The design of digital model-following control systems incorporating fast-sampling PID controllers is described. This methodology is applied to the design of integrated flight-propulsion control systems in which multiple model-following characteristics are achieved explicitly. In this way, it is shown that desired closed-loop airframe responses are achievable simultaneously with desired closed-loop engine responses. These general results are illustrated by designing a digital model-following integrated flight/propulsion control system for a high-performance aircraft with thrust-vectoring and thrust-reversing capabilities.

1. INTRODUCTION

In order to improve the manoeuvring capabilities of next-generation high-performance aircraft, the forces and moments produced by the propulsion system can be used to augment the forces and moments produced by the flight control surfaces. The resultant coupling between the dynamics of the airframe and the dynamics of the propulsion system implies that separate designs of the flight and propulsion control systems are unlikely to be satisfactory. Therefore, in recent years, much effort has been expended on the development of methodologies for the design of integrated flight/propulsion control systems.

However, most of these methodologies[1]–[5] are in fact variations on linear quadratic regulator (LQR) theory. These approaches to the design of integrated flight/propulsion control systems consequently lead to quite complex designs in which model-following characteristics are achieved at best only implicitly. Therefore, in this paper, the methodology of Porter et al[6] for the design of digital model-following control systems is applied to the design of integrated flight/propulsion control systems in which multiple model-following characteristics are achieved explicitly. In this way, it is shown that desired closed-loop airframe response characteristics are achieved simultaneously with desired closed-loop engine response characteristics. Such airframe responses yield excellent flying qualities and are decoupled from engine responses despite the dynamic airframe/engine coupling.

These general results are illustrated by designing a digital model-following integrated flight/propulsion control system for a high-performance aircraft with thrust-vectoring and thrust-reversing capabilities[5]. In this case, it is shown that excellent multiple model-following characteristics are obtained in respect of the pitch rate, angle-of-attack, forward speed, and engine fan speed responses of this aircraft.

2. DIGITAL MODEL-FOLLOWING SYSTEMS

The digital model-following control systems proposed by Porter et al[6] for linear multivariable plants incorporate the following two principal components, as shown in Figure 1:

(*a*) an explicit multivariable dynamical model that generates desired model output vectors, $w(t)$, in response to command input vectors, $v(t)$;

(*b*) a fast-sampling digital PID controller that generates appropriate control input vectors, $u(t)$, in response to errors between model output vectors, $w(t)$, and plant output vectors, $y(t)$.

Such dynamical models may be arbitrarily selected so as to ensure the simultaneous achievement of desired response characteristics in all plant outputs. However, it will be assumed that the linear multivariable plants are governed on the continuous-time set $T = [0,+\infty)$ by state and output equations of the respective forms

$$\dot{x}(t) = Ax(t) + Bu(t) \tag{1}$$

and

$$y(t) = Cx(t) \tag{2}$$

and that the fast-sampling error-actuated PID controllers are governed on the discrete-time set $T_T = \{0,T,2T,\ldots\}$ by control-law equations of the form[6]

$$u(kT) = K_1(T)r(kT) + K_2(T)z(kT) \tag{3}$$

where $T \in R^+$ is the sampling period. Such PID controllers are required to generate the piecewise-constant control input vector $u(t) = u(kT)$, $t \in [kT, (k+1)T)$, $kT \in T_T$, so as to cause the plant output vector $y(t)$ to track the model output vector $w(t)$ on T_T in the sense that the error vector $e(t) = w(t) - y(t)$ assumes the steady-state value

$$\lim_{k\to+\infty} e(kT) = \lim_{k\to+\infty}\{w(kT)-y(kT)\} = 0 \tag{4}$$

for arbitrary initial conditions.

In equations (1), (2), (3), and (4), $x(t) \in R^n$, $u(t) \in R^\ell$, $y(t) \in R^\ell$, $e(t) \in R^\ell$, $w(t) \in R^\ell$, $A \in R^{n\times n}$, $B \in R^{n\times\ell}$, $C \in R^{\ell\times n}$, $r(kT) \in R^\ell$, $z(kT) \in R^\ell$, $K_1(T) \in R^{\ell\times\ell}$, $K_2(T) \in R^{\ell\times\ell}$, and the plant outputs are ordered such that

$$CB = \begin{bmatrix} E_1 & , & E_2 \\ 0_{p,\ell-p} & , & 0_{p,p} \end{bmatrix} \in R^{\ell\times\ell} \tag{5}$$

where $E_1 \in R^{(\ell-p)\times(\ell-p)}$, $E_2 \in R^{(\ell-p)\times p}$, $rank\ E_1 = \ell - p$, and the non-negative integer p is the rank defect of the first Markov parameter of the open-loop plant. Furthermore, $r(kT)$ and $z(kT)$ in equation (3) are generated in accordance with the difference equations[6]

$$s\{(k+1)T\} = -\alpha I_p s(kT) + [0_{p,\ell-p}\ ,\ I_p]e(kT) \quad , \qquad (6a)$$

$$r(kT) = \begin{bmatrix} \frac{2}{T}(1+\alpha)D_2 \\ \\ \frac{2}{T}(1+\alpha)D_4 \end{bmatrix} s(kT) + (I_\ell + \frac{2}{T}D)e(kT),$$

and

$$z\{(k+1)T\} = z(kT) + Tr(kT) \qquad (7)$$

where $\alpha \in (-1,+1]$, $s(kT) \in R^p$, and the derivative matrix

$$D(T) = \begin{bmatrix} 0_{\ell-p,\ell-p}\ ,\ D_2(T) \\ \\ 0_{p,\ell-p}\ \ ,\ D_4(T) \end{bmatrix} \in R^{\ell\times\ell} \qquad (8)$$

is such that[6]

$$D(T)CB = 0_{\ell,\ell} \qquad (9)$$

where $D_2(T) \in R^{(\ell-p)\times p}$ and $D_4(T) \in R^{p\times p}$. In case $p = 0$ (ie, the open-loop plant is regular[6]), the fast-sampling error-actuated digital PID controller governed by equations (3), (6), and (7) clearly reduces to a fast-sampling error-actuated digital PI controller[10].

In terms of the open-loop step-response matrix

$$H(T) = \int^T Ce^{At}B dt \in R^{\ell\times\ell} \qquad (10)$$

and the associated matrix

$$J(T) = H(2T)H^{-1}(T) = \begin{bmatrix} J_1(T),\ J_2(T) \\ \\ J_3(T),\ J_4(T) \end{bmatrix} \in R^{\ell\times\ell} \qquad (11)$$

where $J_1(T) \in R^{(\ell-p)\times(\ell-p)}$, $J_2(T) \in R^{(\ell-p)\times p}$, $J_3(T) \in R^{p\times(\ell-p)}$, and $J_4(T) \in R^{p\times p}$, the appropriate design equations for the PID controller are[6]

$$K_1(T) = TH^{-1}(T)\Sigma(TI_\ell + 2D)^{-1} \quad , \qquad (12)$$

$$K_2(T) = \rho K_1(T) \quad , \qquad (13)$$

and

$$(1+\alpha)\Sigma_1 D_2(T) = J_2(T)\Sigma_2 D_4(T) \quad , \qquad (14)$$

where

$$\Sigma = \begin{bmatrix} \Sigma_1 & , 0_{\ell-p,p} \\ \\ 0_{p,\ell-p} & , \Sigma_2 \end{bmatrix} = \begin{bmatrix} \sigma_1 I_{\ell-p} & , 0_{\ell-p,p} \\ \\ 0_{p,\ell-p} & , \sigma_2 I_p \end{bmatrix} \quad , \qquad (15)$$

$$D_4(T) = \delta_4(T) I_p \quad , \qquad (16)$$

and σ_1, σ_2, ρ, $\sigma_4(T) \in R^+$. The transfer function matrix relating the plant output vector to the model output vector of the closed-loop digital model-following system then assumes the diagonal asymptotic form[6]

$$\Gamma(z) = \begin{bmatrix} \frac{\sigma_1}{z-1+\sigma_1} I_{\ell-p} & , & 0_{\ell-p,p} \\ \\ 0_{p,\ell-p} & , & \frac{\sigma_2(z+1)}{z^2+(\alpha+\sigma_2-1)z+\sigma_2-\alpha} I_p \end{bmatrix} \qquad (17)$$

as the sampling frequency $f = 1/T \to +\infty$, thus indicating that increasingly fast non-interacting behaviour occurs.

In practice, the best choice of design parameters is $\{\sigma_1,\sigma_2,\alpha\} = \{1,1/2,1/2\}$ since it is then evident from equation (17) that all the $\ell+p$ poles of the corresponding asymptotic transfer function matrix

$$\Gamma(z) = \begin{bmatrix} \frac{1}{z} I_{\ell-p} & , 0_{\ell-p,p} \\ \\ 0_{p,\ell-p} & , \frac{z+1}{2z^2} I_p \end{bmatrix} \qquad (18)$$

lie at the origin within D^-. This is because the apparently superior choice $\{\sigma_1,\sigma_2,\alpha\} = \{1,1,1\}$ which would yield

$$\Gamma(z) = \frac{1}{z} I_\ell \qquad (19)$$

is to be avoided since the cancellation of p pairs of discrete-time poles and zeros located at $z = -1$ would lead to undesirable 'ringing' phenomena in the digital model-following system. It then follows directly from equation (18) that, on the discrete-time set T_T,

$$y_k^{(1)} = w_{k-1}^{(1)} \qquad (20)$$

and

$$y_k^{(2)} = \frac{1}{2}(w_{k-1}^{(2)} + w_{k-2}^{(2)}) \quad , \qquad (21)$$

where

$$y_k = \begin{bmatrix} y_k^{(1)} \\ \\ y_k^{(2)} \end{bmatrix} \qquad (22)$$

and

$$w_k = \begin{bmatrix} w_k^{(1)} \\ \\ w_k^{(2)} \end{bmatrix} \qquad (23)$$

in which $y_k^{\{1\}} \in R^{\ell-p}$, $y_k^{\{2\}} \in R^p$, $w_k^{\{1\}} \in R^{\ell-p}$, and $w_k^{\{2\}} \in R^p$. Thus, equation (20) indicates that the plant output vector follows the model output vector by one sampling period in each of the $\ell-p$ closed-loop channels corresponding to those open-loop channels for which the plant is regular (see equation (5)). Similarly, by introducing

$$\varepsilon_k^{(2)} = w_{k-1}^{(2)} - w_{k-2}^{(2)} \quad , \qquad (24)$$

equation (21) becomes

$$y_k^{(2)} = w_{k-2}^{(2)} + {}^1/_2\varepsilon_k^{(2)} \quad , \qquad (25)$$

and therefore indicates that the plant output vector essentially follows the model output vector by two sampling periods in each of the p closed-loop channels corresponding to those open-loop channels for which the plant is irregular (see equation (5)). The vector $\varepsilon_k^{(2)} \in R^p$ in equations (24) and (25) clearly measures the rate of change of the component $w_k^{(2)}$ of the model output vector, and is such that $\varepsilon_k^{(2)}$ vanishes in the case of model output vectors for which $w_k^{(2)}$ becomes constant.

3. INTEGRATED FLIGHT/PROPULSION CONTROL SYSTEM

The linearised longutidinal dynamics of a high-performance aircraft with thrust-vectoring and thrust-reversing capabilities are governed on the continuous-time set $T = [0,+\infty)$ by state and output equations of the respective forms[5]

$$\dot{x}(t) = Ax(t) + Bu(t) \tag{26}$$

and

$$y(t) = Cx(t) \tag{27}$$

In these equations, the state vector

$$x = [x_1 , x_2 , x_3 , x_4 , x_5 , x_6 , x_7 , x_8]^T , \tag{28}$$

the control vector

$$u = [u_1 , u_2 , u_3 , u_4]^T , \tag{29}$$

and the output vector

$$y = [y_1 , y_2 , y_3 , y_4]^T . \tag{30}$$

Here, in the state vector, x_1 = aircraft forward velocity (ft/sec), x_2 = aircraft vertical velocity (ft/sec), x_3 = pitch rate (rad/sec), x_4 = pitch angle (rad), x_5 = engine fan speed (rpm), x_6 = core compressor speed (rpm), x_7 = engine mixing plane pressure ($psia$), x_8 = high-pressure turbine blade temperature ($°R$); in the control vector, u_1 = thrust reverser port area (in^2), u_2 = trailing edge flap deflection less leading edge flap deflection (deg), u_3 = nozzle thrust-vectoring angle (deg), u_4 = engine fuel flow rate (lb/hr); and in the output vector, y_1 = aircraft forward velocity (ft/sec), y_2 = angle of attack (deg), y_3 = generalised pitch rate (deg/sec), y_4 = engine fan speed (% *of maximum allowable speed*). It is important to note that, in order to avoid problems of functional uncontrollability caused by zero-valued transmission zeros[7][8], the generalised pitch rate $x_3 + 0.1\,x_4$ is used for y_3 instead of the pitch rate x_3. The elements of the respective plant, input, and output matrices $A \in R^{8\times8}$, $B \in R^{8\times4}$, and $C \in R^{4\times8}$ are given in the Appendix.

In case the sampling period $T = 0.01\,sec$, the step-response matrix of the open-loop aircraft is

$$H(T) = \begin{bmatrix} -0.212\times10^{2} , & 0.147\times10^{-3}, & -0.861\times10^{-3}, & 0.390\times10^{-6} \\ 0.152\times10^{-6}, & -0.176\times10^{-2}, & -0.582\times10^{-3}, & 0.530\times10^{-10} \\ 0.588\times10^{-4}, & -0.457\times10^{-1}, & 0.504\times10^{-2}, & 0.345\times10^{-7} \\ 0.480\times10^{-2}, & -0.345\times10^{-8}, & -0.404\times10^{-8}, & 0.114\times10^{-4} \end{bmatrix} \tag{31}$$

and the associated matrix defined in equation (11) is

$$J(T) = \begin{bmatrix} 2.043 , & -0.437\times10^{-1}, & -0.479\times10^{-2}, & 0.513\times10^{-2} \\ -0.706\times10^{-3}, & 1.997 , & 0.960\times10^{-2}, & -0.442\times10^{-5} \\ 0.153\times10^{-2}, & 0.131\times10^{-1}, & 1.999 , & 0.365\times10^{-7} \\ -2.491 , & 2.707 , & -0.112 , & 1.991 \end{bmatrix} . \tag{32}$$

This matrix indicates that this aircraft is regular[6] so that $p = 0$ and therefore no derivative action is required in the digital controller. The choices $\sigma_1 = 1$ and $\rho = 1$ in the design equations (12) and (13) yield a fast-sampling error-actuated digital PI controller governed on the discrete-time set $T_T = \{0,T,2T,\ldots\}$ when $T = 0.01\,sec$ by the control law-equation

$$\begin{bmatrix} u_1(kT) \\ u_2(kT) \\ u_3(kT) \\ u_4(kT) \end{bmatrix} = \begin{bmatrix} -0.439\times10^{3} , & 0.477\times10^{3} , & -0.198\times10^{2} , & 0.152\times10^{2} \\ -0.327 , & -0.142\times10^{3} , & -0.164\times10^{2} , & 0.617\times10^{-1} \\ 0.890 , & -0.129\times10^{4} , & 0.497\times10^{2} , & -0.175 \\ 0.185\times10^{6} , & -0.201\times10^{6} , & 0.831\times10^{4} , & 0.814\times10^{5} \end{bmatrix} \begin{bmatrix} e_1(kT) \\ e_2(kT) \\ e_3(kT) \\ e_4(kT) \end{bmatrix}$$

$$+ \begin{bmatrix} -0.439\times10^{3} , & 0.477\times10^{3} , & -0.198\times10^{2} , & 0.152\times10^{2} \\ -0.327 , & -0.142\times10^{3} , & -0.164\times10^{2} , & 0.617\times10^{-1} \\ 0.890 , & -0.129\times10^{4} , & 0.497\times10^{2} , & -0.175 \\ 0.185\times10^{6} , & -0.201\times10^{6} , & 0.831\times10^{4} , & 0.814\times10^{5} \end{bmatrix} \begin{bmatrix} z_1(kT) \\ z_2(kT) \\ z_3(kT) \\ z_4(kT) \end{bmatrix} \tag{33}$$

where $z(kT)$ is generated on T_T in accordance with the vector difference equation

$$\begin{bmatrix} z_1\{(k+1)T\} \\ z_2\{(k+1)T\} \\ z_3\{(k+1)T\} \\ z_4\{(k+1)T\} \end{bmatrix} = \begin{bmatrix} z_1(kT) \\ z_2(kT) \\ z_3(kT) \\ z_4(kT) \end{bmatrix} + 0.01 \begin{bmatrix} e_1(kT) \\ e_2(kT) \\ e_3(kT) \\ e_4(kT) \end{bmatrix} . \tag{34}$$

The outputs of the digitally controlled aircraft are shown in Figure 2 in response to a command input vector $v = [10\,ft/sec\ ,\ 1\,deg\ ,\ 0.5\,deg/sec\ ,\ 30\%]^T$, and the corresponding control inputs are shown in Figure 3. This closed-loop behaviour is obtained by selecting models with the respective transfer functions

$$m_1 = \frac{1}{\tau_U s+1} , \tag{35}$$

$$m_2 = \frac{K_\alpha}{(s^2+2\zeta\omega s+\omega^2)} , \tag{36}$$

$$m_3 = \left(1+\frac{0.1}{s}\right)\frac{K_q\left(s+\frac{1}{\tau_{\theta_2}}\right)}{(s^2+2\zeta\omega s+\omega^2)} \quad , \qquad (37)$$

and

$$m_4 = \frac{1}{\tau_N s+1} \quad , \qquad (38)$$

in the forward-speed, angle-of-attack, generalised pitch-rate, and engine-speed channels, where $\tau_U = 1$, $K_\alpha = 5.01$, $\zeta = 0.89$, $\omega = 2.24$, $K_q = 10.02$, $1/\tau_{\theta_2} = 0.5$, and $\tau_N = 0.1$. Indeed, the actual multiple model-following responses of the aircraft in respect of forward speed, angle of attack, generalised pitch rate, and engine speed shown in Figure 2 are indistinguishable from the desired responses implied by these models.

In this way, it is seen that the desired closed-loop airframe response characteristics are achieved simultaneously with the desired engine response characteristics. These airframe responses yield excellent flying qualities (in consonance with military specifications) which are decoupled from the engine responses despite the dynamic airframe/engine coupling indicated by equations (26) and (27). Indeed, as shown in Figure 4(a), the flight path angle lags the pitch angle by τ_{θ_2} *secs* in precisely the manner specified by the model governed by equation (37) whilst, as shown in Figure 4(b), the angle of attack and the pitch rate are such that $y_2 = \tau_{\theta_2} x_3$ in the steady-state in precisely the manner specified by the models governed by equations (36) and (37).

4. CONCLUSION

The methodology of Porter et al[6] for the design of digital model-following systems has been applied to the design of integrated flight/propulsion control systems in which multiple model-following characteristics are achieved explicitly. In this way, it has been shown that desired closed-loop airframe responses are achievable simultaneously with desired closed-loop engine responses. These general results have been illustrated by designing a digital model-following integrated flight/propulsion control system for a high-performance aircraft with thrust-vectoring and thrust-reversing capabilities.

REFERENCES

(1) P D Shaw, S M Rock, and W S Fisk, "Design methods for integrated control systems", AFWAL-TR-88-2061, Aero Propulsion Laboratory, Air Force Wright Aeronautical Laboratories, Dayton, Ohio, June 1988.

(2) S M Rock, A Emami-Naeini, and R P Anex, "Propulsion control specifications in integrated flight-propulsion control systems", AIAA Paper No 88-3236, AIAA/ASME/SAE/ASEE 24th Joint Propulsion Conference, Boston, Mass, 1988.

(3) K L Smith, "Design methods for integrated control systems", AFWAL-TR-88-2103, Aero Propulsion Laboratory, Air Force Wright Aeronautical Laboratories, Dayton, Ohio, December 1986.

(4) S Garg, D L Mattern, and R E Bullard, "Integrated flight/propulsion control system design based on a centralised approach", AIAA Paper No 89-3520, AIAA Guidance, Navigation and Control Conference, Boston, Mass, 1989.

(5) D K Schmidt and J D Schierman, "Extended implicit model-following as applied to integrated flight and propulsion control", AIAA Paper No 90-3444, AIAA Guidance, Navigation and Control Conference, Portland, Oregon, 1990.

(6) B Porter, A Manganas, and T Manganas, "Design of digital model-following flight-mode control systems for high-performance aircraft", AIAA Paper No 88-4116, AIAA Guidance, Navigation and Control Conference, Minneapolis, Minnesota, 1988.

(7) B Porter and H M Power, "Controllability of multivariable systems incorporating integral feedback", Electron Lett, Vol 6, pp 689-690, 1970.

(8) H M Power and B Porter, "Necessary and sufficient conditions for controllability of multivariable systems incorporating integral feedback", Electron Lett, Vol 6, pp 815-816, 1970.

APPENDIX

The plant, input, and output matrices for the nominal high-performance aircraft with thrust-vectoring and thrust-reversing capabilities[5] are as follows:

$$A = \begin{bmatrix}
-5.893e{-2}, & 1.067e{-1}, & -3.860e{+1}, & -3.184e{+1}, & 3.144e{-4}, \\
-2.659e{-1}, & -2.665e{-1}, & 1.948e{+2}, & -4.599e{+0}, & -1.578e{-5}, \\
-1.541e{-3}, & 7.806e{-3}, & -1.949e{-1}, & -4.818e{-4}, & 9.460e{-7}, \\
0 & 0 & 1.000e{+0}, & 0 & 0 \\
7.782e{-1}, & 1.542e{-1}, & 0 & 0 & -4.191e{+0}, \\
1.518e{-1}, & 3.008e{-2}, & 0 & 0 & 4.263e{-1}, \\
7.934e{-1}, & 1.572e{-1}, & 0 & 0 & 2.295e{-1}, \\
-1.005e{-1}, & -1.992e{-2}, & 0 & 0 & 3.740e{-2},
\end{bmatrix}$$

$$\begin{bmatrix}
2.599e{-4}, & 3.819e{-2}, & 2.250e{-3} \\
-2.106e{-6}, & 1.826e{-4}, & -2.957e{-6} \\
3.744e{-7}, & 3.668e{-5}, & 2.676e{-6} \\
0 & 0 & 0 \\
6.022e{+0}, & -3.434e{+2}, & 1.160e{+1} \\
-5.707e{+0}, & 2.716e{+1}, & 1.040e{+1} \\
1.155e{-1}, & -9.024e{+1}, & 8.476e{-1} \\
-1.036e{-1}, & -7.954e{+1}, & -1.068e{+0}
\end{bmatrix},$$

$$B = \begin{bmatrix}
-2.055e{-1}, & -4.183e{-4}, & -8.428e{-2}, & 3.436e{-5} \\
-2.936e{-4}, & -5.452e{-1}, & -2.147e{-1}, & 1.238e{-8} \\
1.068e{-4}, & -7.970e{-2}, & 8.813e{-3}, & 5.507e{-8} \\
0 & 0 & 0 & 0 \\
0 & 0 & 0 & 1.469e{-1} \\
0 & 0 & 0 & 5.360e{-2} \\
-4.302e{+1}, & 0 & 0 & 1.813e{-2} \\
0 & 0 & 0 & 1.643e{-1}
\end{bmatrix},$$

and

$$C = \begin{bmatrix}
1.000e{+0}, & 0 & 0 & 0 & 0 & 0,0,0 \\
0 & 2.830e{-1}, & 0 & 0 & 0 & 0,0,0 \\
0 & 0 & 5.730e{+1}, & 5.730e{+0}, & 0 & 0,0,0 \\
0 & 0 & 0 & 0 & 8.723e{-3} & 0,0,0
\end{bmatrix}.$$

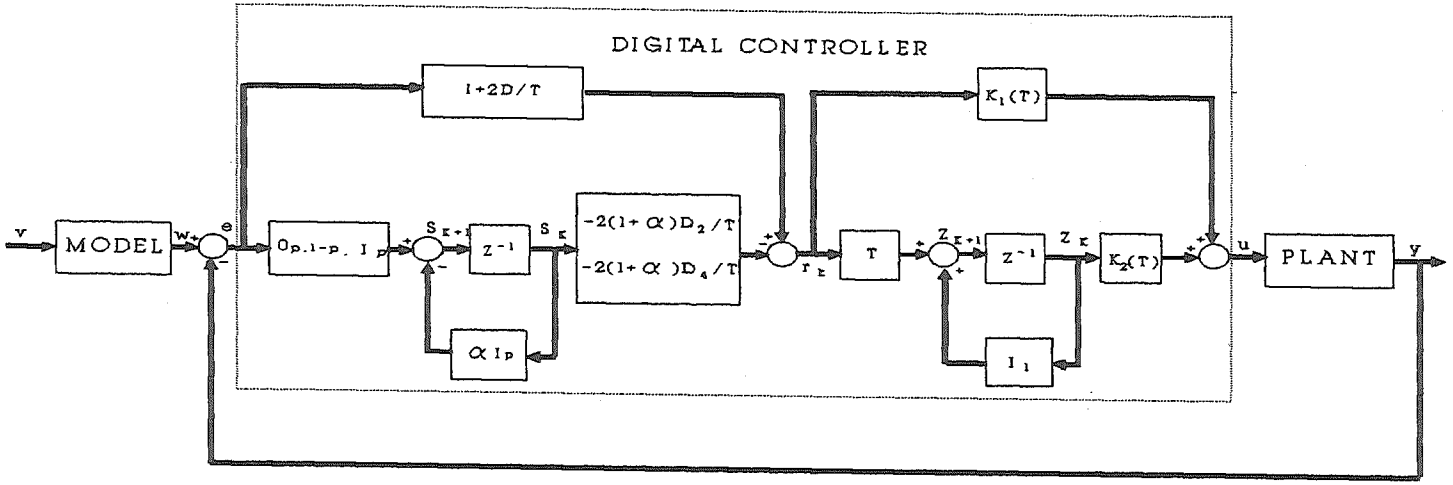

Fig.1 Block diagram of digital model-following control system.

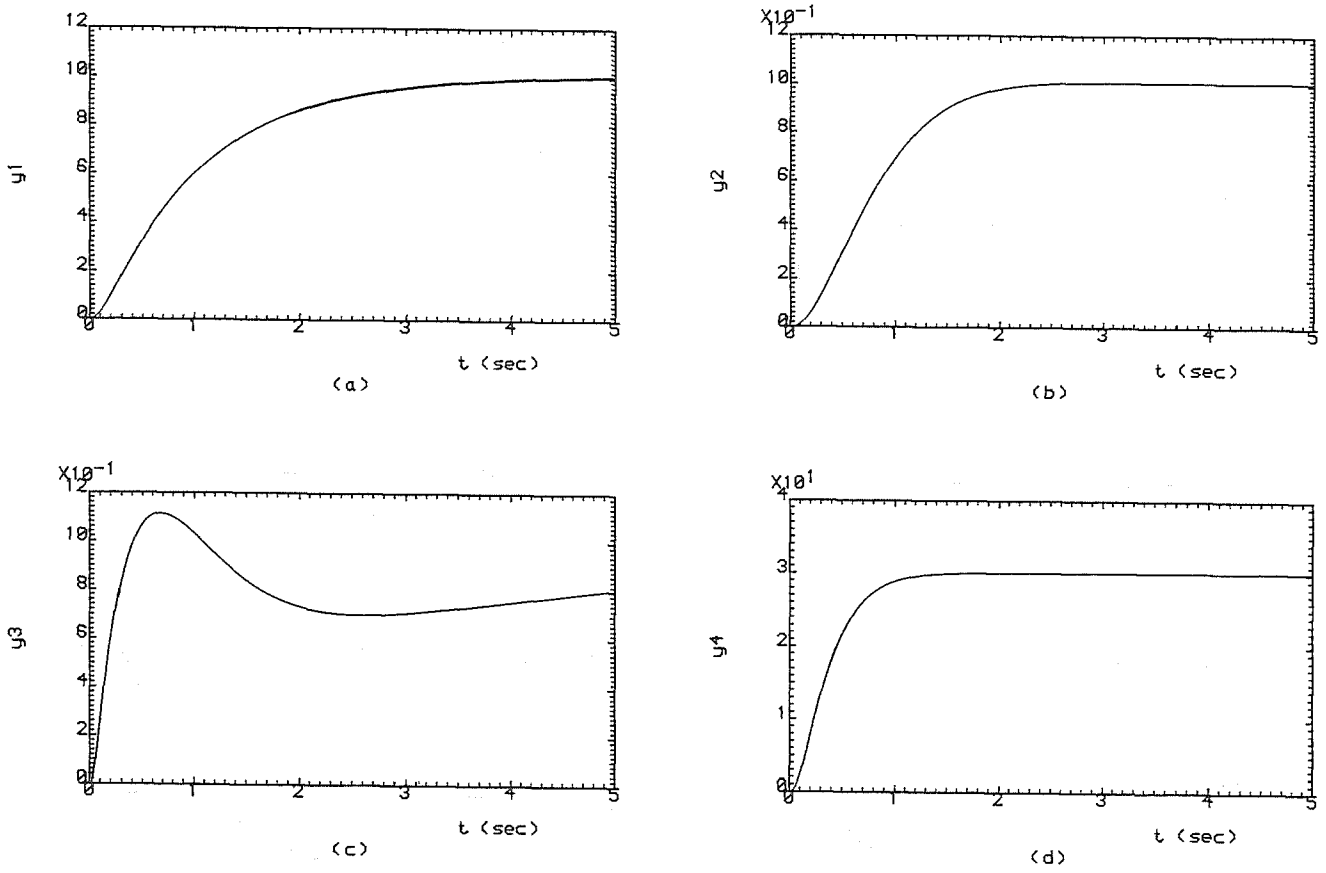

Fig.2: Multiple model-following outputs of digitally controlled aircraft

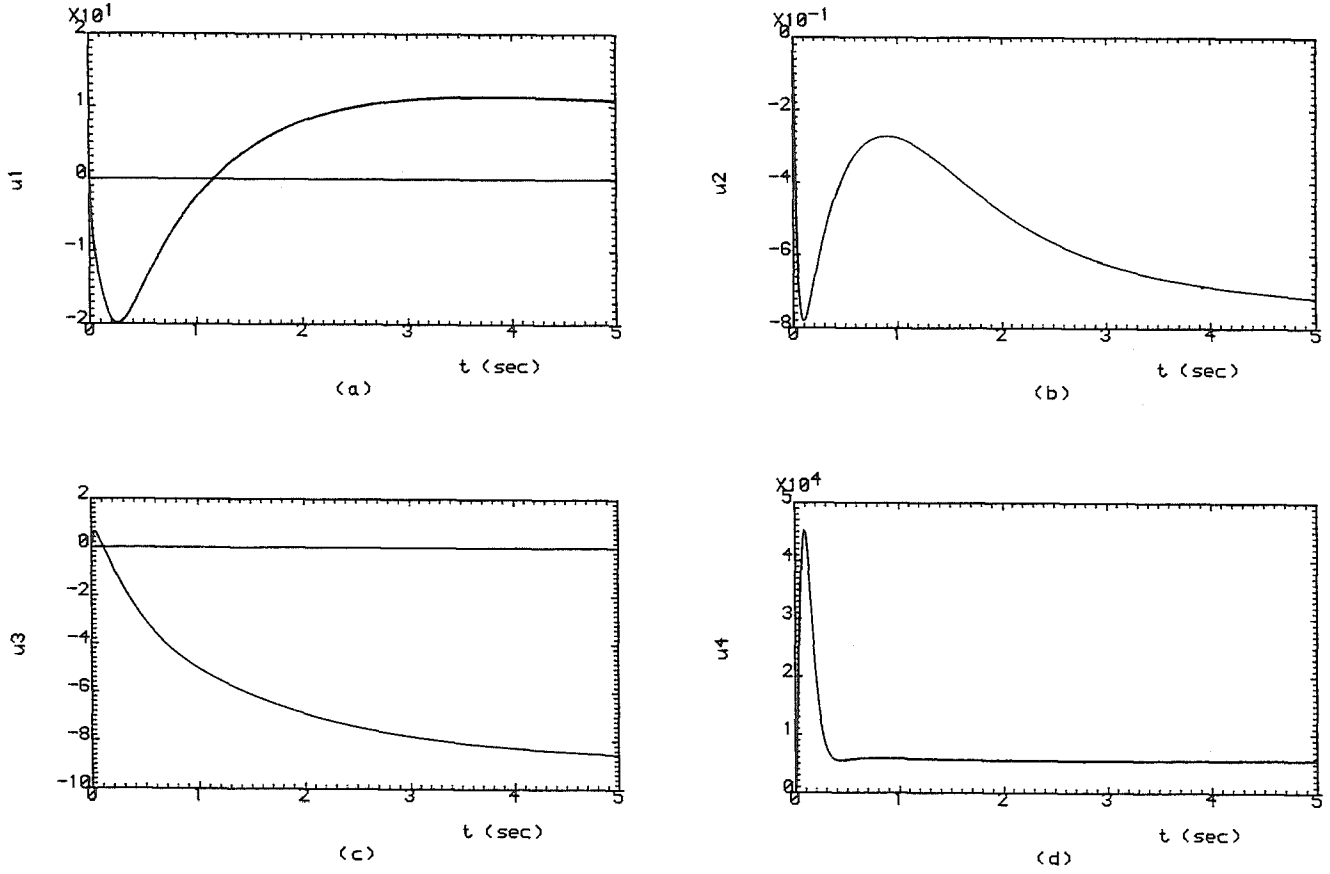

Fig.3: Control inputs of digitally controlled aircraft

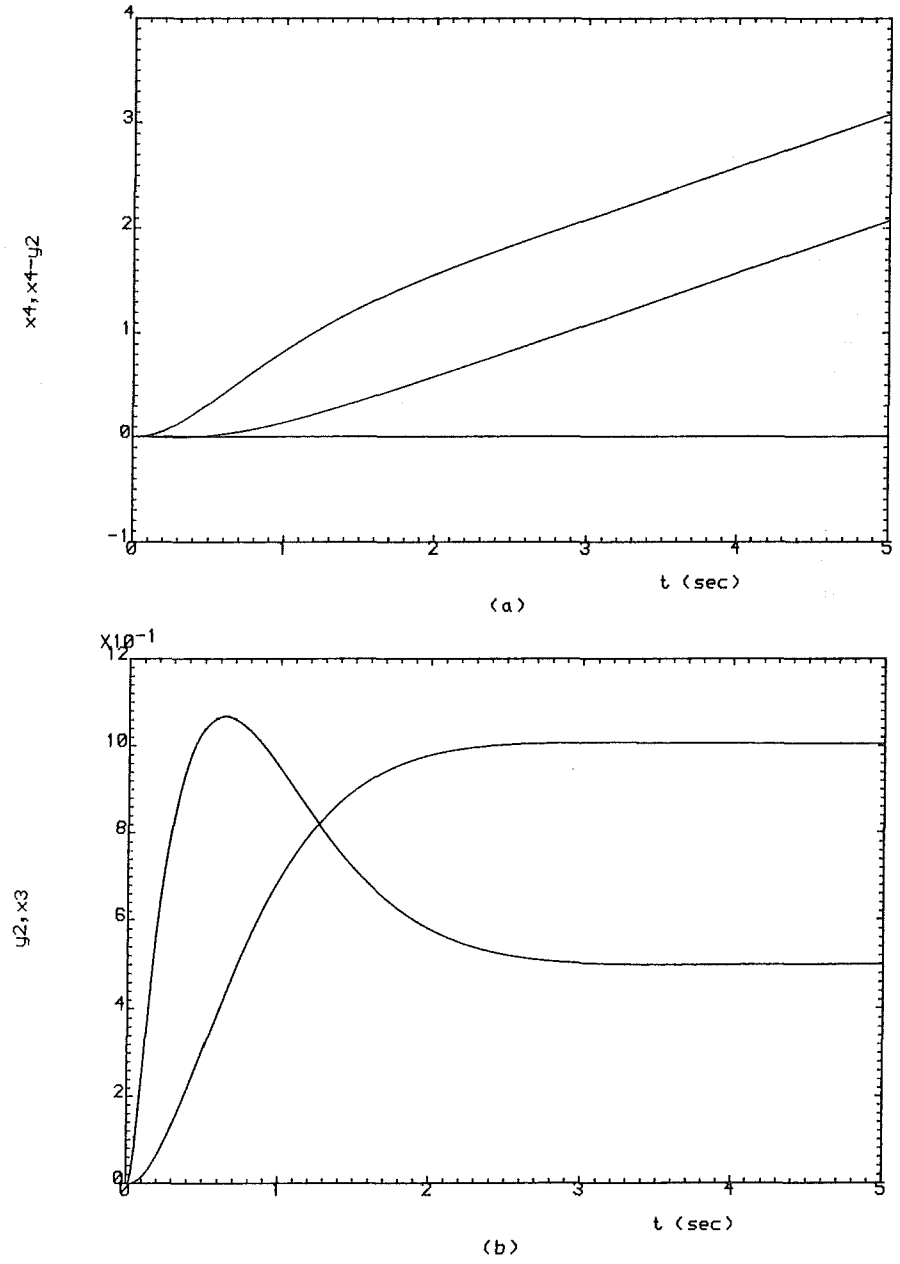

Fig.4: Airframe responses of digitally controlled aircraft